Spatially Correlated RIS-Aided CF Massive MIMO Systems With Generalized MR Combining

Enyu Shi, *Graduate Student Member, IEEE*, Jiayi Zhang, *Senior Member, IEEE*, Ying Du, Zhiqin Wang, Bo Ai, *Fellow, IEEE*, and Derrick Wing Kwan Ng, *Fellow, IEEE*

***Abstract*—In this correspondence, we study the uplink ergodic net throughput of a spatially correlated reconfigurable intelligent surface (RIS)-aided cell-free (CF) massive multiple-input multiple-output (MIMO) system over Rayleigh fading channels. We investigate the impact of the generalized maximum ratio (GMR) combining and obtain the closed-form expression for characterizing the uplink net throughput revealing that the GMR can double the system performance compared with the maximum ratio (MR) in our system. Then, we compare the performance and complexity of the MR, GMR, and large-scale fading decoding (LSFD). Moreover, we consider a practical fractional power control to mitigate the inter-user interference. The obtained interesting results show that the system performance decreases with the increasing number of RIS elements. It reveals that efficient interference cancellation processing is needed to cope with severer pilot contamination brought by the large number of RIS elements to improve the system performance. Finally, the accuracy of our derived analytical results has been verified by Monte-Carlo simulations.**

***Index Terms*—Reconfigurable intelligent surface, cell-free massive MIMO, generalized maximum ratio, spatial correlation, fractional power control.**

I. Introduction

Cell-free (CF) massive multiple-input multiple-output (MIMO) has recently been introduced as a promising future technology for enabling beyond-5G wireless communication systems [1]. However, in some practical scenarios with harsh communication environments such as large obstructions or poor scattering environments, the received signal strength may drop sharply and the promised CF Massive MIMO gain cannot be achieved for quality of service (QoS) provisioning [2]. Meanwhile, reconfigurable intelligent surface (RIS) has recently emerged as a promising new technology to realize reconfigurable wireless channels/radio propagation environment [3]–[6]. Specifically, with massive reflective and refractive elements at RIS, effective passive beamforming can be performed by altering the phase of the reflected impinging signals. Besides, RIS has the advantages of low power and low cost which can be flexibly deployed assisting users with poor channel conditions to improve communication quality [7]–[9].

Recently, to further increase the capacity of CF network, the combination of CF massive MIMO and RIS has been advocated by leveraging their individual advantages jointly. For example, in [10], the authors proposed a joint precoding framework for RIS-aided CF massive MIMO systems to improve the system capacity, which designs an alternating optimization-based scheme to address the non-convex RIS beamforming problem. Furthermore, in [11] the authors introduced an RIS-aided CF wireless energy transfer framework to improve the system energy efficiency and the communication quality. However, none of the aforementioned studies considered the existence of spatial correlation of RIS elements that may affect the system performance [12]. To handle this problem, the authors in [2] proposed an aggregated channel estimation method and considered the performance of a single spatial correlation RIS-assisted CF massive MIMO systems. Although the use of the maximum ratio (MR) combining at the CPU in [2] has low computational complexity, its performance is unsatisfactory. On the other hand, one can utilize the minimum mean square error (MMSE) scheme at the AP for improving the system performance. Yet, it incurs exceedingly high computational complexity due to the involved high-dimensional matrix inversion [13]. In particular, when a RIS is equipped with a large number of elements, the computational complexity increases exponentially, which places higher demands on the CPU hardware. Thus, it is necessary to apply a low-complexity processing method that can improve system performance. For this reason, in [14], the authors proposed the generalized maximum ratio (GMR) combining in CF massive MIMO which only requires the large-scale fading information while it can significantly improve the system performance compared to the MR.

In this work, motivated by the aforementioned observations, we study the uplink throughput of RIS-aided CF massive MIMO systems under spatially correlated channels with GMR combining at CPU. More specifically, we derive closed-form expressions for analyzing the uplink net throughput of the considered system. The results reveal that the GMR not only enjoys low complexity, but also offers a significant performance improvement compared with the MR. In particular, we find that the system throughput decreases with the increasing number of RIS elements. Indeed, both pilot contamination and inter-user interference increase with the number of RIS elements while GMR combining can only harness the magnified interference to a certain extent. Then, we compare the performance and complexity of the MR, GMR, and large-scale fading decoding (LSFD). Finally, we propose a practical and simple fractional power control (FPC) scheme to enhance the overall system performance.

II. System Model

We consider an RIS-aided CF massive MIMO system consisting of M APs, one RIS, and K UEs. We assume that all APs and UEs

Manuscript received 16 January 2022; revised 13 May 2022; accepted 19 June 2022. Date of publication 24 June 2022; date of current version 17 October 2022. This work was supported in part by National Key R&D Program of China under Grant 2020YFB1806903, in part by the National Natural Science Foundation of China under Grant 61971027, in part by Beijing Natural Science Foundation under Grant L202013, in part by Frontiers Science Center for Smart High-speed Railway System. The work of D. W. K. Ng was supported by the Australian Research Council's Discovery Project under Grant DP210102169. The review of this article was coordinated by Prof. Yue Gao. *(Corresponding authors: Zhiqin Wang; Jiayi Zhang.)*

Enyu Shi and Jiayi Zhang are with the School of Electronics and Information Engineering, Beijing Jiaotong University, Beijing 100044, China, and also with the Frontiers Science Center for Smart High-speed Railway System, Beijing Jiaotong University, Beijing 100044, China (e-mail: 21111047@bjtu.edu.cn; jiayizhang@bjtu.edu.cn).

Ying Du and Zhiqin Wang are with the China Academy of Information and Communications Technology, Beijing 100191, China (e-mail: duying1@caict.ac.cn; zhiqin.wang@caict.ac.cn).

Bo Ai is with the State Key Laboratory of Rail Traffic Control and Safety, Beijing Jiaotong University, Beijing 100044, China, also with the Frontiers Science Center for Smart High-speed Railway System, Beijing Jiaotong University, Beijing 100044, China, also with the Henan Joint International Research Laboratory of Intelligent Networking and Data Analysis, Zhengzhou University, Zhengzhou 450001, China, and also with the Research Center of Networks and Communications, Peng Cheng Laboratory, Shenzhen 518000, China (e-mail: boai@bjtu.edu.cn).

Derrick Wing Kwan Ng is with the School of Electrical Engineering and Telecommunications, University of New South Wales, NSW 2052, Australia (e-mail: w.k.ng@unsw.edu.au).

Digital Object Identifier 10.1109/TVT.2022.3186077

are equipped with a single antenna and RIS has N reflective elements which can alter the phases of the reflected impinging signals. All APs are connected to a CPU via fronthaul links. Without loss of generality, we adopt the standard time division duplex (TDD) protocol in the system, where τ_c is the length of each coherence block. We assume that τ_p symbols are utilized for the channel estimation phase and $\tau_c - \tau_p$ symbols are used for the uplink and downlink data transmission phases.

The direct channel between AP m and UE k is $g_{mk} \in \mathbb{C}$. Variable $\mathbf{h}_m \in \mathbb{C}^N$ is the channel from AP m to the RIS and $\mathbf{z}_k \in \mathbb{C}^N$ denotes the channel from the RIS to UE k. Here, we consider a realistic spatial correlated channel model among the RIS elements, which is due to the elements sub-wavelength structure [12]. Since CF is mainly deployed in urban scenarios with abundant scattering paths, we apply Rayleigh fading to model the AP-UE, AP-RIS, and RIS-UE channels [2]. As such, the corresponding channel distributions of g_{mk}, $\mathbf{h}_m$, and $\mathbf{z}_k$ are given by

$$g_{mk} \sim \mathcal{CN}\left(0, \beta_{mk}\right), \tag{1}$$

$$\mathbf{h}_m \sim \mathcal{CN}\left(\mathbf{0}, \mathbf{R}_m\right), \mathbf{z}_k \sim \mathcal{CN}\left(\mathbf{0}, \tilde{\mathbf{R}}_k\right), \tag{2}$$

respectively, where β_{mk} is the large-scale fading coefficient between AP m and UE k. $\mathbf{R}_m \in \mathbb{C}^{N\times N}$ and $\tilde{\mathbf{R}}_k \in \mathbb{C}^{N\times N}$ are the spatial covariance matrices given by [12]

$$\mathbf{R}_m = \alpha_m A\mathbf{R},\ \tilde{\mathbf{R}}_k = \tilde{\alpha}_k A\mathbf{R}, \tag{3}$$

respectively, where $\alpha_m, \tilde{\alpha}_k$ are the large-scale fading coefficients and $A = d_H d_V$ denotes the area of each element of the RIS. d_V and d_H are the vertical height and the horizontal width of each element, respectively. In particular, the matrix $\mathbf{R} \in \mathbb{C}^{N\times N}$ characterizes the spatial correlation of RIS which has the $(m,' n')$-th element as $[\mathbf{R}]_{m'n'} = \mathrm{sinc}(2\|\mathbf{u}_{m'} - \mathbf{u}_{n'}\|/\lambda)$, where λ denotes the carrier wavelength and $\mathrm{sinc}(x) = \sin(\pi x)/(\pi x)$ denotes the sinc function. Besides, $\mathbf{u}_x = [0, \mathrm{mod}(x-1, N_H)d_H, \lfloor (x-1)/N_H \rfloor d_V]^T$, $x \in \{m,' n'\}$ is the position vector, where N_H and N_V denote the number of elements in each row and column, respectively, such that $N = N_H \times N_V$, and $\mathrm{mod}(\cdot,\cdot)$ is the modulus operation. In this article, we assume that the RIS is designed as a square structure, while its numbers of rows and columns are equal, i.e., $d_H = d_V$ and $N_H = N_V$.

The RIS phase shift matrix is written as $\mathbf{\Phi} = \mathrm{diag}\left(e^{j\theta_1}, e^{j\theta_2}, \ldots, e^{j\theta_N}\right)$, where $\theta_n \in [-\pi, \pi], \forall n \in \{1, \ldots, N\}$ is the phase shift of the nth RIS element. Thus, the total uplink channel between UE k and AP m is given by

$$u_{mk} = g_{mk} + \mathbf{h}_m^H \mathbf{\Phi} \mathbf{z}_k, \forall m, k, \tag{4}$$

which consists of a direct link between AP m and UE k and a cascaded link reflected by the RIS.

A. Uplink Channel Estimation

We estimate the channels independently based on the τ_p pilot sequence transmitted by the K UEs in each coherence block. All UEs share the τ_p orthogonal pilot sequences. In particular, $\boldsymbol{\phi}_k \in \mathbb{C}^{\tau_p \times 1}$ is the pilot sequence of UE k and satisfies $\|\boldsymbol{\phi}_k\|^2 = 1$. Let $\mathcal{P}_k$ denotes the index subset of UEs which adopts the same pilot sequence as UE k, including itself. Specifically, UE k transmits the pilot sequence $\sqrt{\tau_p}\boldsymbol{\phi}_k$ and all K UEs send the pilot sequences to all the M APs during the uplink channel estimation phase. Stacking the received pilot signals from all UEs at AP m as $\mathbf{y}_m^p \in \mathbb{C}^{\tau_p \times 1}$:

$$\mathbf{y}_m^p = \sum_{k=1}^{K} \sqrt{p\tau_p} u_{mk} \boldsymbol{\phi}_k + \mathbf{n}_m^p, \tag{5}$$

where p is the normalized signal-to-noise ratio (SNR) of each pilot symbol and $\mathbf{n}_m^p \in \mathbb{C}^{\tau_p \times 1}$ is the additive noise and is modeled as $\mathbf{n}_m^p \sim \mathcal{CN}(\mathbf{0}, \mathbf{I}_{\tau_p})$. By multiplying the received signal by $\boldsymbol{\phi}_k^H$ at AP m, we can obtain the results for UE k as

$$y_{mk}^p = \boldsymbol{\phi}_k^H \mathbf{y}_m^p = \sqrt{p\tau_p} u_{mk} + \sum_{k' \in \mathcal{P}_k \setminus \{k\}} \sqrt{p\tau_p} u_{mk'} + n_{mk}^p, \tag{6}$$

where $n_{mk}^p = \boldsymbol{\phi}_k^H \mathbf{n}_m^p \sim \mathcal{CN}(0,1)$. We assume that the MMSE channel estimator is used at AP m. From (6), the estimation of u_{mk} can be derived as

$$\hat{u}_{mk} = \left(\mathbb{E}\left\{(y_{mk}^p)^* u_{mk}\right\} y_{mk}^p\right) \Big/ \mathbb{E}\left\{|y_{mk}^p|^2\right\} = c_{mk} y_{mk}^p, \tag{7}$$

where c_{mk} can be obtained as

$$c_{mk} = \frac{\sqrt{p\tau_p}\delta_{mk}}{p\tau_p \sum_{k' \in \mathcal{P}_k} \delta_{mk'} + 1}, \tag{8}$$

where $\delta_{mk} = \mathbb{E}\{|u_{mk}|^2\} = \beta_{mk} + \mathrm{tr}(\mathbf{\Theta}_{mk})$ denotes the second moment of channel u_{mk} and $\mathbf{\Theta}_{mk} = \mathbf{\Phi}^H \mathbf{R}_m \mathbf{\Phi} \tilde{\mathbf{R}}_k$ [2]. The $\mathbb{E}\{\cdot\}$ and $\mathrm{tr}(\cdot)$ denote the Euclidean norm and the trace operator, respectively. The estimated channel $\hat{u}_{mk}$ has zero mean and the variance is expressed as

$$\gamma_{mk} = \mathbb{E}\left\{|\hat{u}_{mk}|^2\right\} = \sqrt{p\tau_p}\delta_{mk} c_{mk}. \tag{9}$$

The mean of the estimation error $\tilde{u}_{mk} = u_{mk} - \hat{u}_{mk}$ is zero and its variance can be written as

$$\mathbb{E}\left\{|\tilde{u}_{mk}|^2\right\} = \delta_{mk} - \gamma_{mk}. \tag{10}$$

Note that y_{mk}^p varies across different coherence blocks, whereas δ_{mk} stay as a constant for the longer period time. Also, the estimated channel $\hat{u}_{mk}$ and the error $\tilde{u}_{mk}$ of estimated channel are uncorrelated but not independent.

B. Uplink Data Transmission

In this subsection, we consider the uplink data transmission, where the UEs transmit the uplink data to all APs simultaneously. Then, the received signal at AP m is given by

$$y_m^u = \sqrt{\rho_u} \sum_{k=1}^{K} \sqrt{\eta_k} u_{mk} s_k + n_m^u, \tag{11}$$

where ρ_u is the normalized SNR of each uplink data symbol. η_k denotes the power control coefficient with $0 \le \eta_k \le 1$, which is set according to the large-scale fading information to enhance the spectral efficiency and will be designed later. $s_k \sim \mathcal{CN}(0,1)$ denotes the uplink signal of UE k and $n_m^u \sim \mathcal{CN}(0,1)$ denotes the normalized additive noise. We assume that the considered system adopts the centralized processing and all APs directly convey the received signals to the CPU for joint decoding [15]. Different from the previous work in [15], [16], the CPU adopts the GMR combining method, i.e., $v_{mk} = w_{mk}\hat{u}_{mk}$, where w_{mk} is the GMR coefficient given later to obtain the uplink data transmission

symbol by UE k and the combined received signal at the CPU can be derived by

$$\begin{aligned} r_k^u &= \sum_{m=1}^{M} v_{mk}^* y_m^u \\ &= \underbrace{\sqrt{\rho_u} \sum_{k' \in \mathcal{P}_k} \sum_{m=1}^{M} \sqrt{\eta_{k'}} w_{mk}^* \hat{u}_{mk}^* u_{mk'} s_{k'}}_{\Gamma_1} \\ &+ \underbrace{\sqrt{\rho_u} \sum_{k' \notin \mathcal{P}_k} \sum_{m=1}^{M} \sqrt{\eta_{k'}} w_{mk}^* \hat{u}_{mk}^* u_{mk'} s_{k'}}_{\Gamma_2} + \underbrace{\sum_{m=1}^{M} w_{mk}^* \hat{u}_{mk}^* n_m^u}_{\Gamma_3}, \end{aligned} \tag{12}$$

where Γ_1 denotes the signals received from all UEs in $\mathcal{P}_k$ which includes the pilot contamination and Γ_2 denotes the mutual interference from the UEs that are allocated different pilots with UE k. Γ_3 reveals the effect of noise after the GMR combining method.

III. Performance Analysis

In this section, we study the uplink performance of the RIS-aided CF massive MIMO system and investigate the impact of GMR combining. In addition, we propose a practical and simple FPC algorithm for the considered system to enhance the system uplink throughput.

A. Uplink Ergodic Net Throughput

The uplink ergodic net throughput lower bound of UE k can be obtained by utilizing the use-and-then-forget (UatF) bound [13] as follows

$$R_k^u = B v_u \left(1 - \frac{\tau_p}{\tau_c}\right) \log_2 \left(1 + \gamma_k^u\right), \tag{13}$$

where B denotes the bandwidth of the system. v_u denotes the proportion of each coherence time interval used for the uplink data transmission. The effective signal-to-interference-plus-noise ratio (SINR) γ_k^u can be written as follows

$$\gamma_k^u = \frac{|\mathrm{DS}_k^u|^2}{\mathbb{E}\left\{|\mathrm{BU}_k^u|^2\right\} + \sum_{k'=1, k' \neq k}^{K} \mathbb{E}\left\{|\mathrm{UI}_{k'k}^u|^2\right\} + \mathbb{E}\left\{|\mathrm{NO}_k^u|^2\right\}}, \tag{14}$$

where

$$\mathrm{DS}_k^u = \sqrt{\rho_u \eta_k} \mathbb{E}\left\{\sum_{m=1}^{M} v_{mk}^* u_{mk}\right\}, \tag{15}$$

$$\mathrm{BU}_k^u = \sqrt{\rho_u \eta_k} \left(\sum_{m=1}^{M} v_{mk}^* u_{mk} - \mathbb{E}\left\{\sum_{m=1}^{M} v_{mk}^* u_{mk}\right\}\right), \tag{16}$$

$$\mathrm{UI}_{k'k}^u = \sqrt{\rho_u \eta_{k'}} \sum_{m=1}^{M} v_{mk}^* u_{mk'}, \tag{17}$$

$$\mathrm{NO}_k^u = \sum_{m=1}^{M} v_{mk}^* n_m^u. \tag{18}$$

In particular, DS_k^u represents the strength of the desired signal, BU_k^u represents the uncertainty of beamforming due to the imperfect channel state information (CSI), $\mathrm{UI}_{k'k}^u$ denotes the interference between UE k and UE k', and NO_k^u represents the additive noise after combining.

Note that the closed-form expression for the uplink net throughput is proved in [2] if the MR combining method is utilized at the CPU, which is a baseline method for comparison in the following section. In contrast, we assume that the CPU applies the GMR combining method [14], i.e., $v_{mk} = w_{mk} \hat{u}_{mk}$. We derive the closed-form expression of (14) in Theorem 1.

Theorem 1: The closed-form expression for the uplink net throughput of UE k is given by (13), where the SINR is expressed as (19) shown at the bottom of this page.

Proof: The proof is given in Appendix A. ■

Remark We note that in (19), the number of RIS elements affects both the numerator and the denominator of the SINR. When the RIS element number increases, the equivalent large-scale fading coefficient δ_{mk} of each UE is improved. Hence, the symbol power received by each AP becomes stronger for each UE, so as the inter-user interference. In particular, the MR/GMR combining method cannot effectively eliminate the interference between UEs. Therefore, in RIS-aided CF systems, it applying advanced interference cancellation processing is needed to cope with the increasing number of RIS elements to improve the performance.

B. Power Control

In general, the system performance is limited by the near-far effects. As a remedy, we extend the FPC scheme proposed in [17] to the considered RIS-aided CF massive MIMO system. Specifically, the FPC scheme for the RIS-aided CF massive MIMO system relies on the equivalent large-scale fading coefficients for the current UE, which capture the connection strength from the UE to all the APs. Inspired by this, we select the power control factor of UE k as

$$\eta_k = \left(\frac{\min\limits_k \left(\sum_{m=1}^{M} \varepsilon_{mk} \delta_{mk}\right)}{\sum_{m=1}^{M} \varepsilon_{mk} \delta_{mk}}\right)^{\alpha}, \forall k, \tag{20}$$

where δ_{mk} is given in (8) and $0 < \alpha < 1$ denotes the fractional power control parameter. ε_{mk} takes different values according to the MR and GMR combining method, which are 1 and w_{mk} respectively. For uplink transmission, we pay more attention to the fairness of UEs and (20) aims to improve the performance of UEs with poor connection strength.

IV. Numerical Results and Discussion

In this section, some numerical results are provided to verify and evaluate the performance of the RIS-aided CF massive MIMO systems.

$$\gamma_k^u = \frac{\rho_u \eta_k \left(\sum\limits_{m=1}^{M} w_{mk} \gamma_{mk}\right)^2}{\begin{aligned} &\rho_u \sum_{k'=1}^{K} \sum_{m=1}^{M} \eta_{k'} w_{mk}^2 \gamma_{mk} \delta_{mk'} + p \tau_p \rho_u \sum_{k'=1}^{K} \sum_{k'' \in \mathcal{P}_k} \sum_{m=1}^{M} \sum_{m'=1}^{M} \eta_{k'} w_{mk} w_{m'k} c_{mk} c_{m'k} \mathrm{tr}\left(\boldsymbol{\Theta}_{mk'} \boldsymbol{\Theta}_{m'k''}\right) \\ &+ \rho_u p \tau_p \sum_{k' \in \mathcal{P}_k} \sum_{m=1}^{M} \eta_{k'} w_{mk}^2 c_{mk}^2 \mathrm{tr}\left(\boldsymbol{\Theta}_{mk'}^2\right) + \rho_u p \tau_p \sum_{k' \in \mathcal{P}_k \setminus \{k\}} \eta_{k'} \left(\sum_{m=1}^{M} w_{mk} c_{mk} \delta_{mk'}\right)^2 + \sum_{m=1}^{M} w_{mk}^2 \gamma_{mk} \end{aligned}}. \tag{19}$$

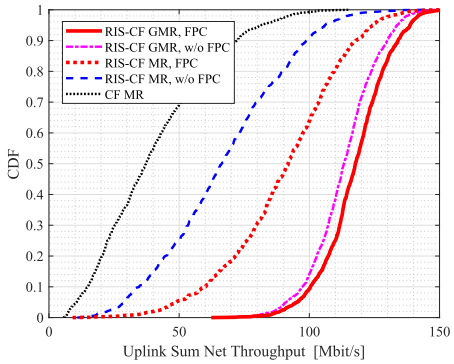

Fig. 1. CDF of the uplink sum net throughput against different systems with the MR and GMR combining methods ($M = 40$, $K = 10$, $N = 36$, $\tau_p = 5$, $d_{\mathrm{V}} = \frac{1}{2}\lambda$).

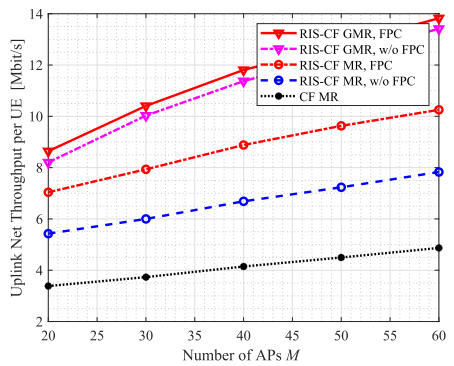

Fig. 2. Uplink net throughput per UE versus the different number of APs against different systems with the MR and GMR ($K = 10$, $N = 36$, $\tau_p = 5$, $d_{\mathrm{V}} = \frac{1}{2}\lambda$).

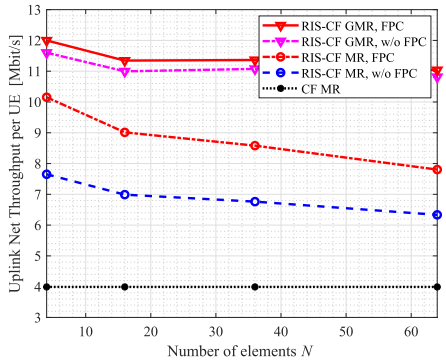

Fig. 3. Uplink net throughput per UE versus the different number of RIS elements against different systems with the MR and GMR ($M = 40$, $K = 10$, $\tau_p = 5$, $d_{\mathrm{V}} = \frac{1}{2}\lambda$).

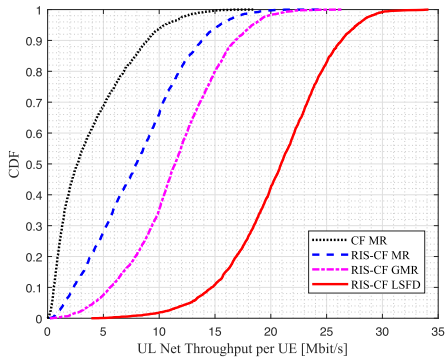

Fig. 4. CDF of the uplink net throughput per UE against different systems with the MR, GMR combining methods, and LSFD ($M = 40$, $K = 10$, $N = 36$, $\tau_p = 5$, $d_{\mathrm{V}} = \frac{1}{2}\lambda$).

We assume that APs and UEs are uniformly distributed within an $1 \times 1\,\mathrm{km}^2$ square area using the wrap-around deployment. The RIS is deployed at the regional center. We set the carrier frequency is 1.9GHz. Besides, each coherence block consists of $\tau_c = 200$ corresponding to a coherence bandwidth of 200 kHz and $\tau_p = 5$ are reserved for pilot transmission. We adopt the three-slope propagation model in [18] to generate the large-scale fading coefficients with the log-normal shadow fading with standard deviation 8 dB and the three slopes distance thresholds are 10 m and 50 m. Without loss of generality, we set the height of UEs, RIS, and APs as 1.65 m, 30 m, and 15 m, respectively. The coefficient v_u for each coherence time interval used for the uplink data transmission is 0.5. The noise power is -92 dBm corresponding to the noise figure as 9 dB. All UEs transmit uplink pilots and data with 100 mW and 200 mW. Besides, the uplink power control coefficient is obtained in (20) and the fractional power control parameters α of MR and GMR are 1 and 0.5 [17], respectively. As for the phase shift design, the N elements phase shift is set equal to $\pi/4$.

Fig. 1 compares the CDF of the uplink sum net throughput for RIS-aided CF massive MIMO and CF massive MIMO systems under random UE and AP locations with the MR/GMR combining and FPC. It is clear that the RIS-aided CF system has a significant gain over the CF system. Meanwhile, GMR combining achieves a 1.7 times improvement at the median compared with MR. When applying FPC, the performance of MR can be improved by 1.6 times at 95%-likely points. In contrast, FPC only brings a slight performance improvement to GMR.

Fig. 2 shows the uplink net throughput per UE as the function of the number of APs M for different systems. It is clear that in the fixed setting, the per UE uplink net throughput increases with the number of APs M increases. In particular, the system performance with GMR improves more significantly than MR. This reveals that in the RIS-aided CF systems with GMR, we can always improve system performance by increasing the number of APs as it can shorten the potential communication distance between desired transceivers.

An interesting finding is shown in Fig. 3, that the effect of the RIS elements number N on the per UE throughput. When increasing the number of RIS elements, the performance of the RIS-aided CF system decreases whereas the decline of GMR combining is less than that of MR. This is because as the number of RIS elements increases, the increase of δ_{mk} also leads to an increase in pilot contamination during the channel estimation phase. Meanwhile, as the equivalent channels of all UEs have been improved during the uplink data transmission phase, interference among UEs has also increased as explained in Remark 1. This is a problem caused by the CF system architecture with distributed APs and more efficient processing methods, e.g., interference cancellation, that need to be considered to enhance the system throughput.

Fig. 4 compares the CDF of the uplink net throughput per UE with the MR/GMR combining and LSFD strategy. It is clear that the RIS-aided CF system achieves a significant gain over the LSFD strategy. The weight coefficient of LSFD can maximize the SE, as it is calculated from the global CSI. However, the complexities for complex multiplications

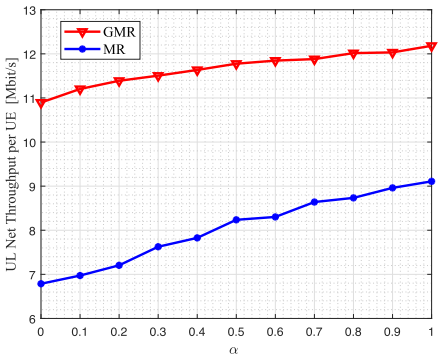

Fig. 5. CDF of the uplink net throughput per UE against different α with the MR and GMR combining methods ($M = 40$, $K = 10$, $N = 36$, $\tau_p = 5$, $d_{\mathrm{V}} = \frac{1}{2}\lambda$).

of the LSFD are $\mathcal{O}(\frac{1}{3}M^3 + (K + \frac{3}{2})M^2 + \frac{13}{6}M)$ [13], which is much higher than that of the GMR $\mathcal{O}((4\tilde{K} + 1)M)$. Therefore, the GMR serves as a compromise approach that strikes a balance between complexity and the system performance, especially in CF massive MIMO systems with a large number of APs.

Fig. 5 shows the uplink net throughput per UE as the function of α with the MR and GMR combining. It is clear that the system average net throughput increases as the FPC parameter increases. However, the proposed FPC only brings a slight performance improvement to the GMR, since the optimized combining coefficients in the GMR have already exploited most of the performance gain from the large-scale information.

V. Conclusion

In this correspondence, we investigated the uplink performance of the spatially correlated RIS-aided CF massive MIMO systems with the GMR combining. We first derived the closed-form expression of the uplink ergodic net throughput of the considered system to analyze the system performance. We found that compared with the MR, the GMR combining can significantly improve the system performance. Besides, the FPC scheme was proposed to improve the system performance in both the MR and GMR. Importantly, we found an interesting result that with the increasing number of RIS elements, the system performance decreases. In future work, we will consider the beamforming design and spatial correlation of multi-antenna APs to enable the implementation of RIS-aided CF massive MIMO networks.

Appendix A
Proof of Theorem 1

The w_{mk} in (19) denotes the m-th diagonal element of matrix $\mathbf{W}_k$ which related to large-scale information as [19]

$$\mathbf{W}_k = \mathbf{Q}_k^{-1}\left(\sum_{i=1}^{K} a_{ki}\mathbf{\Lambda}_i\right)\mathbf{\Lambda}_k^{-1}, \tag{21}$$

where $\mathbf{Q}_k = \sum_{i=1}^{K}\mathbf{\Lambda}_i + \frac{1}{\rho_u}\mathbf{I}_M$ and $\mathbf{\Lambda}_k = \mathrm{diag}(\delta_{1k}, \delta_{2k}, \ldots, \delta_{Mk})$. a_{ki} is the (k,i)-th element of the matrix $(\mathbf{A} + \frac{1}{M}\mathbf{I}_M)^{-1}$ and $\mathbf{A}$ is given by

$$[\mathbf{A}]_{ki} = \frac{1}{M}\sum_{m=1}^{M}\frac{\delta_{mk}\delta_{mi}}{\left(\sum_{i=1}^{K}\delta_{mi} + \frac{1}{p}\right)\left(\sum_{i=1}^{K}\delta_{mi} + \frac{1}{\rho_u}\right)}. \tag{22}$$

With GMR combining $v_{mk} = w_{mk}\hat{u}_{mk}$, the desired signal strength is equal to

$$|\mathrm{DS}_k^u|^2 = \left(\sqrt{\rho_u\eta_k}\mathbb{E}\left\{\sum_{m=1}^{M} w_{mk}^*\hat{u}_{mk}^* u_{mk}\right\}\right)^2$$
$$\overset{(a)}{=}\rho_u\eta_k\left(\sum_{m=1}^{M} w_{mk}^*\gamma_{mk}\right)^2. \tag{23}$$

(a) is obtained because the estimated channel and the channel estimation error are uncorrelated. The beamforming uncertainty (16) can be written as

$$\mathbb{E}\left\{|\mathrm{BU}_k^u|^2\right\} = \rho_u\eta_k\mathbb{E}\left\{\left|\sum_{m=1}^{M}\chi_{mk}\right|^2\right\}$$
$$= \underbrace{\rho_u\eta_k\sum_{m=1}^{M}\sum_{m'=1,m'\neq m}^{M}\mathbb{E}\left\{\chi_{mk}\chi_{m'k}^*\right\}}_{T_0} + \underbrace{\rho_u\eta_k\sum_{m=1}^{M}\mathbb{E}\left\{|\chi_{mk}|^2\right\}}_{T_1},$$

where $\chi_{mk} = w_{mk}^*\hat{u}_{mk}^* u_{mk} - \mathbb{E}\{w_{mk}^*\hat{u}_{mk}^* u_{mk}\}$. Similar to [2], T_0 and T_1 can be computed and the expression of the beamforming uncertainty as follows

$$\mathbb{E}\left\{|\mathrm{BU}_k^u|^2\right\} = \rho_u\eta_k\sum_{m=1}^{M} w_{mk}^2\gamma_{mk}\delta_{mk}$$
$$+\rho_u\eta_k\sum_{m=1}^{M} p\tau_p w_{mk}^2 c_{mk}^2\mathrm{tr}\left(\mathbf{\Theta}_{mk}^2\right) + p\tau_p\rho_u\eta_k\sum_{k''\in\mathcal{P}_k}$$
$$\times\sum_{m=1}^{M}\sum_{m'=1}^{M} c_{mk}c_{m'k}w_{mk}^* w_{m'k}\mathrm{tr}\left(\mathbf{\Theta}_{mk}\mathbf{\Theta}_{m'k''}\right). \tag{24}$$

According to the repeated pilot set defined in $\mathcal{P}_k$, we can divide the second term in the denominator of (14) into two terms as follows

$$\sum_{k'=1,k'\neq k}^{K}\mathbb{E}\left\{|\mathrm{UI}_{k'k}^u|^2\right\} = \sum_{k'\notin\mathcal{P}_k}\mathbb{E}\left\{|\mathrm{UI}_{k'k}^u|^2\right\} + \sum_{k'\in\mathcal{P}_k\setminus\{k\}}\mathbb{E}\left\{|\mathrm{UI}_{k'k}^u|^2\right\}.$$

Finally, we calculate the additive noise in (14) as follows

$$\mathbb{E}\left\{|\mathrm{NO}_{UK}|^2\right\} = \sum_{m=1}^{M}\mathbb{E}\left\{|w_{mk}^*\hat{u}_{mk}^* n_m^u|^2\right\} = \sum_{m=1}^{M} w_{mk}^2\gamma_{mk}. \tag{25}$$

Substituting the above results into (14) with the aid of some algebraic manipulations and the results follow immediately.

References

[1] J. Zhang, E. Björnson, M. Matthaiou, D. W. K. Ng, H. Yang, and D. J. Love, "Prospective multiple antenna technologies for beyond 5G," *IEEE J. Sel. Areas Commun.*, vol. 38, no. 8, pp. 1637–1660, Aug. 2020.

[2] T. Van Chien, H. Q. Ngo, S. Chatzinotas, M. Di Renzo, and B. Ottersten, "Reconfigurable intelligent surface-assisted cell-free massive MIMO systems over spatially-correlated channels," *IEEE Trans. Wireless Commun.*, early access, Dec. 29, 2021, doi: 10.1109/TWC.2021.3136925.

[3] Q. Wu and R. Zhang, "Toward smart and reconfigurable environment: Intelligent reflecting surface aided wireless network," *IEEE Commun. Mag.*, vol. 58, no. 1, pp. 106–112, Jan. 2020.

[4] B. Di, H. Zhang, L. Song, Y. Li, Z. Han, and H. V. Poor, "Hybrid beamforming for reconfigurable intelligent surface based multiuser communications: Achievable rates with limited discrete phase shifts," *IEEE J. Sel. Areas Commun.*, vol. 38, no. 8, pp. 1809–1822, Aug. 2020.

[5] J. Zhang et al., "RIS-aided next-generation high-speed train communications: Challenges, solutions, and future directions," *IEEE Wireless Commun.*, vol. 28, no. 6, pp. 145–151, Dec. 2021.
[6] Y. Jin et al., "Multiple residual dense networks for reconfigurable intelligent surfaces cascaded channel estimation," *IEEE Trans. Veh. Technol.*, vol. 71, no. 2, pp. 2134–2139, Feb. 2022.
[7] Q. Wu and R. Zhang, "Intelligent reflecting surface enhanced wireless network via joint active and passive beamforming," *IEEE Trans. Wireless Commun.*, vol. 18, no. 11, pp. 5394–5409, Nov. 2019.
[8] M. Di Renzo et al., "Smart radio environments empowered by reconfigurable intelligent surfaces: How it works, state of research, and the road ahead," *IEEE J. Sel. Areas Commun.*, vol. 38, no. 11, pp. 2450–2525, Nov. 2020.
[9] Y. Zhang, J. Zhang, M. Di Renzo, H. Xiao, and B. Ai, "Reconfigurable intelligent surfaces with outdated channel state information: Centralized vs. distributed deployments," *IEEE Trans. Commun.*, vol. 26, no. 1, pp. 2742–2756, Apr. 2022.
[10] Z. Zhang and L. Dai, "A joint precoding framework for wideband reconfigurable intelligent surface-aided cell-free network," *IEEE Trans. Signal Process.*, vol. 69, no. 6, pp. 4085–4101, Jun. 2021.
[11] E. Shi et al., "Wireless energy transfer in RIS-aided cell-free massive MIMO systems: Opportunities and challenges," *IEEE Commun. Mag.*, vol. 60, no. 3, pp. 26–32, Mar. 2022.
[12] E. Björnson and L. Sanguinetti, "Rayleigh fading modeling and channel hardening for reconfigurable intelligent surfaces," *IEEE Wireless Commun. Lett.*, vol. 10, no. 4, pp. 830–834, Apr. 2021.
[13] E. Björnson and L. Sanguinetti, "Making cell-free massive MIMO competitive with MMSE processing and centralized implementation," *IEEE Trans. Wireless Commun.*, vol. 19, no. 1, pp. 77–90, Jan. 2020.
[14] A. Á. Polegre, L. Sanguinetti, and A. G. Armada, "Pilot decontamination processing in cell-free massive MIMO," *IEEE Commun. Lett.*, vol. 25, no. 12, pp. 3990–3994, Dec. 2021.
[15] J. Zhang, J. Zhang, D. W. K. Ng, S. Jin, and B. Ai, "Improving sum-rate of cell-free massive MIMO with expanded compute-and-forward," *IEEE Trans. Signal Process.*, vol. 70, no. 11, pp. 202–215, Nov. 2022.
[16] Z. Wang, J. Zhang, B. Ai, C. Yuen, and M. Debbah, "Uplink performance of cell-free massive MIMO with multiantenna users over jointly-correlated rayleigh fading channels," *IEEE Trans. Wireless Commun*., early access, Mar. 17, 2022, doi: 10.1109/TWC.2022.3158353.
[17] R. Nikbakht and A. Lozano, "Uplink fractional power control for cell-free wireless networks," in *Proc. IEEE Int. Conf. Commun.*, 2019, pp. 1–5.
[18] H. Q. Ngo, A. Ashikhmin, H. Yang, E. G. Larsson, and T. L. Marzetta, "Cell-free massive MIMO versus small cells," *IEEE Trans. Wireless Commun.*, vol. 16, no. 3, pp. 1834–1850, Mar. 2017.
[19] L. Sanguinetti, E. Björnson, and J. Hoydis, "Toward massive MIMO 2.0: Understanding spatial correlation, interference suppression, and pilot contamination," *IEEE Trans. Commun.*, vol. 68, no. 1, pp. 232–257, Jan. 2020.